AIAA JOURNAL
Vol. 43, No. 12, December 2005

Analysis and Stabilization of Fluid–Structure Interaction Algorithm for Rigid-Body Motion

Jan Vierendeels,* Kris Dumont,† Erik Dick,‡ and Pascal Verdonck§
Ghent University, B-9000 Ghent, Belgium

Fluid–structure interaction computations in geometries where different chambers are almost completely separated from each other by a movable rigid body but connected through very small gaps can encounter stability problems when a standard explicit coupling procedure is used for the coupling of the fluid flow and the movement of the rigid body. An example of such kind of flows is the opening and closing of valves, when the valve motion is driven by the flow. A stability analysis is performed for the coupling procedure of the movement of a cylinder in a cylindrical tube, filled with fluid. Between the moving cylinder and the tube, a small gap is present, so that two chambers are formed. It is shown that a standard explicit coupling procedure or an implicit coupling procedure with explicit coupling in the subiterations steps can lead to unstable motion depending on the size of the gaps, the density of the rigid body, and the density of the fluid. It is proven that a reduction of the time-step size cannot stabilize the coupling procedure. An implicit coupling procedure with implicit coupling in the subiterations has to be used. An illustration is given on how such a coupling procedure can be implemented in a commercial computational fluid dynamics (CFD) software package. The CFD package FLUENT (Fluent, Inc.) is used. As an application, the opening and the closing of a prosthetic aortic valve is computed.

Introduction

FLUID–STRUCTURE interaction (FSI) problems with moving valves are popular in biomedical applications where the simulation of the flow in the heart during the cardiac cycle is one of the goals to be achieved. Different coupling methods for this FSI problem have been used. Both in the immersed boundary method[1,2] and in the fictitious domain method[3–5] a fixed grid is used for the flow calculation. The influence of the structure is introduced by momentum sources in the momentum equations of the flow. However, if details of the flow around the valves are of interest, for example, shear stresses, it would be more appropriate to use an arbitrary Lagrangian–Eulerian (ALE) method because the accuracy of the latter method is better in the vicinity of the moving boundaries for a given mesh density. Makhijani et al. presented a real three-dimensional simulation of a pericardial bioprosthetic aortic valve during the complete cardiac cycle.[6] They used an implicit "influence coefficient" technique to couple the flow with the motion of the structure.

In this paper, different coupling procedures for the motion of a rigid body in a moving fluid are analyzed analytically and numerically. Different time-integration schemes for the motion of the valve are compared. First, a stability analysis is performed for the coupling procedure of the movement of a cylinder in a cylindrical tube, filled with fluid. Between the moving cylinder and the tube, a small gap is present, so that two chambers are formed. It is shown that the coupling procedure for this kind of problem is representative for the rigid-valve motion during opening and closing. The valve motion is coupled with the flow motion computed with the commercial computational fluid dynamics (CFD) software package FLUENT (Fluent, Inc.). The dynamic mesh model of FLUENT 6.1 has been used for the ALE computations.

Received 8 July 2003; revision received 30 January 2004; presented as Paper 2005-4703 at the AIAA 17th Computational Fluid Dynamics Conference, Toronto, ON, Canada, 6–9 June 2005; accepted for publication 7 July 2005.

*Professor, Department of Flow, Heat and Combustion Mechanics, Sint Pietersnieuwstraat 41; Jan.Vierendeels@UGent.be. Member AIAA.
†Research Fellow, IBiTech, Institute of Biomedical Technology, Hydraulics Laboratory, Sint Pietersnieuwstraat 41.
‡Professor, Department of Flow, Heat and Combustion Mechanics, Sint Pietersnieuwstraat 41. Member AIAA.
§Professor, IBiTech, Institute of Biomedical Technology, Hydraulics Laboratory, Sint Pietersnieuwstraat 41.

Stability Analysis for a Generic One-Dimensional Test Case

Definition of the Test Case

As a generic one-dimensional test case for the kind of FSI problem treated in this paper, a moving cylinder is considered in a cylindrical tube (Fig. 1). Between the cylinder and the tube there exists a small gap that connects the fluid at the front and the back of the cylinder. There exists an analogy between the moving valve problem and the one-dimensional test case because during certain phases of the valve motion a small gap also is present that connects the fluid on both sides of the valve. Also, both problems are described with one degree of freedom. In Fig. 1, $u(t)$ is the velocity of the oncoming fluid, $v(t)$ is the velocity in the gaps, $\dot{x}$ is the velocity of the rigid body, and A and A_b are the cross-sectional area of the tube and the front area of the rigid body, respectively.

For this generic test case, the conservation of mass is given by

$$Au(t) = A_b\dot{x}(t) + (A - A_b)v(t) \tag{1}$$

or

$$v(t) = (1/a)[u(t) - (1 - a)\dot{x}(t)] \tag{2}$$

with $a = A_g/A$ and $A_g = A - A_b$.

The conservation of momentum in the gap is

$$\frac{\partial v}{\partial t} + \frac{1}{\rho_f}\frac{\partial p}{\partial x} = 0 \tag{3}$$

for inviscid flow. Here ρ_f is the density of the fluid, and p is the pressure. In the analysis, the influence of the viscous terms is neglected. The driving force for the rigid-body motion is given by the pressure difference between the left and right wall of the cylinder. This pressure difference is

$$p_l - p_r = \frac{\partial v}{\partial t}L\rho_f \tag{4}$$

with L the length of the gap. The force on the solid body is then given by

$$F = A_b(p_l - p_r) = (1 - a)A(p_l - p_r) \tag{5}$$

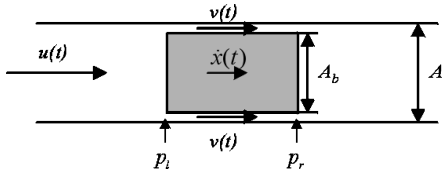

Fig. 1 Motion of a rigid body in a tube, generic one-dimensional test case.

The equation of motion for the solid body becomes

$$m\ddot{x} = F \tag{6}$$

or

$$\ddot{x} = \frac{\partial u}{\partial t}\frac{\rho_f}{\rho_s}\frac{1}{a} - \ddot{x}\frac{1-a}{a}\frac{\rho_f}{\rho_s} \tag{7}$$

with ρ_s the density of the solid.

Discretization

Because a commercial package is used for the fluid calculation, the interface characteristics of this software have to be taken into account. The fluid solver uses an ALE algorithm. Thus, starting from a known state at time level n, the new position of the boundary at time level $n+1$ has to be provided. With the other boundary conditions given as a function of the time, for example, at inlet and outlet, the software computes a new state on time level $n+1$. The time-discretization scheme that can be selected for the ALE calculations in FLUENT is only the backward Euler scheme. Therefore, the fluid discretization part of the generic one-dimensional test case problem is also done with a backward Euler approach. Notice that only the position x is the variable that is passed through the interface between the solid and the fluid problem and is common for both problems. It means that both problems have their own variables for the other state variables, for example, velocity. With a backward Euler discretization, the force F^{n+1} is given by

$$\begin{aligned} F^{n+1}/m &= (\rho_f/\rho_s)[(v^{n+1}-v^n)/\Delta t] \\ &= (\rho_f/\rho_s)\Big\{(1/a)[(u^{n+1}-u^n)/\Delta t] \\ &\quad -[(1-a)/a]\Big[\big(\dot{x}_{\mathrm{NS}}^{n+1}-\dot{x}_{\mathrm{NS}}^{n}\big)/\Delta t\Big]\Big\} \end{aligned} \tag{8}$$

Note that the velocity used in the Navier–Stokes solver is denoted as $\dot{x}_{\mathrm{NS}}$. This velocity can be related to the position vector x as

$$\dot{x}_{\mathrm{NS}}^{n+1} = [(x^{n+1}-x^n)/\Delta t] \tag{9}$$

again using the backward Euler discretization of the Navier–Stokes solver. The force is then passed to the solid problem and used in the equation of motion

$$m\ddot{x}^{n+1} = F^{n+1} \tag{10}$$

Here $\ddot{x}$ is the acceleration variable in the solid problem. The equation of motion can be integrated to obtain the velocity $\dot{x}^{n+1}$ of the solid problem and the position x^{n+1}. We consider a class of integration schemes given by

$$\begin{aligned} \dot{x}^{n+1} &= \dot{x}^n + (1-\beta)\ddot{x}^n\Delta t + \beta\ddot{x}^{n+1}\Delta t \\ x^{n+1} &= x^n + \dot{x}^n\Delta t + \gamma\ddot{x}^n\Delta t^2 + \alpha\ddot{x}^{n+1}\Delta t^2 \end{aligned} \tag{11}$$

For $\gamma = 1/2-\alpha$, this corresponds to the class of Newmark schemes. For $\gamma=0$ and $\alpha=\beta=1$, this corresponds to the backward Euler scheme. Indeed, with the latter choice, the scheme can be rewritten as

$$\dot{x}^{n+1} = \dot{x}^n + \ddot{x}^{n+1}\Delta t, \qquad x^{n+1} = x^n + \dot{x}^{n+1}\Delta t \tag{12}$$

From Eqs. (8–11), F^{n+1} and the variable x^n and x^{n+1} can be eliminated easily. The resulting equations can be written in matrix form:

$$\begin{aligned} \begin{bmatrix} 0 & 1 & -\alpha \\ 1 & 0 & -\beta \\ 0 & K & 1 \end{bmatrix} \begin{bmatrix} \dot{x}\Delta t \\ \dot{x}_{\mathrm{NS}}\Delta t \\ \ddot{x}\Delta t^2 \end{bmatrix}^{n+1} &= \begin{bmatrix} 1 & 0 & \gamma \\ 1 & 0 & 1-\beta \\ 0 & K & 0 \end{bmatrix} \begin{bmatrix} \dot{x}\Delta t \\ \dot{x}_{\mathrm{NS}}\Delta t \\ \ddot{x}\Delta t^2 \end{bmatrix}^{n} \\ &\quad + \begin{bmatrix} 0 \\ 0 \\ \dfrac{K}{1-\alpha}(u^{n+1}-u^n)\Delta t \end{bmatrix} \end{aligned} \tag{13}$$

where K is given by

$$K = (\rho_f/\rho_s)[(1-a)/a] \tag{14}$$

Equation (13) can be rewritten is condensed form as

$$A\phi^{n+1} = B\phi^n + D \tag{15}$$

Stability of the Time-Integration Scheme

The time-integration scheme (15) is stable if the amplitude of all eigenvalues of the matrix $C = A^{-1}B$ is not larger than one. The characteristic equation for the eigenvalues λ_i of C is given by

$$\begin{aligned} &(\lambda-1)\{\lambda^2 - [(\alpha-\beta-\gamma)K/(1+\alpha K)]\lambda \\ &\qquad + (1-\beta-\gamma)K/(1+\alpha K)\} = 0 \end{aligned} \tag{16}$$

The eigenvalues λ_i are

$$\lambda_1 = 1$$

$$\lambda_{2,3} = \frac{(\alpha-\beta-\gamma)K \pm \sqrt{(\alpha+\beta+\gamma)^2K^2 - 4K(1+\alpha K-\beta-\gamma)}}{2(1+\alpha K)} \tag{17}$$

The eigenvector corresponding to the eigenvalue 1 is $[1\ 1\ 0]^T$. It is seen, if u is constant in time ($D=[0\ \ 0\ \ 0]^T$), that the solution of the generic test case corresponds with a motion at constant speed. This solution corresponds to the eigenmode with eigenvalue 1, that is,

$$\begin{bmatrix} \dot{x} \\ \dot{x}_{\mathrm{NS}} \\ \ddot{x} \end{bmatrix}^{n+1} = \begin{bmatrix} \dot{x} \\ \dot{x}_{\mathrm{NS}} \\ \ddot{x} \end{bmatrix}^{n} \tag{18}$$

if $\dot{x}^n = \dot{x}_{\mathrm{NS}}^n$ and $\ddot{x}^n = 0$. The other modes are spurious and should be damped. They are formed by a linear combination of, for example, a mode corresponding with a different speed in the solid and the fluid problem and no acceleration ($[1\ \ -1\ \ 0]^T$) and a mode with velocity zero and an acceleration different from zero ($[0\ \ 0\ \ 1]^T$). Note that the two latter modes are not necessarily eigenmodes, but form a span for these eigenmodes. Thus, to damp the spurious modes, the amplitude of the eigenvalues λ_2 and λ_3 must be strictly smaller than one and for good damping close to zero.

With the transformation

$$\lambda_i = (1+z_i)/(1-z_i) \tag{19}$$

the inner part of the unit circle in the λ plane is transformed into the left half-plane of the z plane. After elimination of the factor $(\lambda-1)$ in Eq. (16), the transformation gives

$$\begin{aligned} &[1+K(1+2\alpha-2\beta-2\gamma)]z^2 \\ &\qquad + 2[1+K(\alpha+\beta+\gamma-1)]z + 1 + K = 0 \end{aligned} \tag{20}$$

or

$$a_2z^2 + a_1z + a_0 = 0 \tag{21}$$

The conditions for stability are now that $\Re(z_i) \leq 0$ (Routh–Hurwitz conditions). For a quadratic polynomial, these are fulfilled if a_0, a_1, and a_2 have the same sign. The stability conditions are given by

$$1 + K(1 + 2\alpha - 2\beta - 2\gamma) > 0$$
$$1 + K(\alpha + \beta + \gamma - 1) > 0 \tag{22}$$

For large, but finite, values of K, the conditions are

$$\beta + \gamma \leq \alpha + \tfrac{1}{2}, \qquad \alpha + \beta + \gamma \geq 1 \tag{23}$$

Note that solutions can be found only if $\alpha \geq \frac{1}{4}$.

Choice of the Time Integration Scheme

An explicit scheme for the motion of the solid is obtained for $\alpha = \beta = 0$. Conditions for γ can then be fulfilled only if $K < 3$. This means that for large K an explicit scheme is unstable and cannot be used.

A Newmark scheme is obtained if $\gamma = \frac{1}{2} - \alpha$. For large K, the stability conditions are $2\alpha \geq \beta \geq \frac{1}{2}$. A Newmark scheme is second-order accurate in time (see Ref. 7) if $\beta = \frac{1}{2}$. The product of the eigenvalues λ_2 and λ_3 are given by the constant in Eq. (16) after elimination of the factor $(\lambda - 1)$. For the second-order Newmark scheme, this constant is equal to $\alpha K/(1 + \alpha K)$, which is very close to one for large values of K. Thus, the second-order Newmark scheme has almost no damping for the spurious modes arising in the generic test case problem. A typical choice for α for a second-order Newmark scheme is $\alpha = \frac{1}{4}$. The eigenvalues are then given by

$$\lambda_{2,3} = \left(-K \pm 2i\sqrt{K}\right)\Big/(K + 4) \tag{24}$$

which are close to -1 for large K. Therefore, for this choice of parameters ($\alpha = \frac{1}{4}$, $\beta = \frac{1}{2}$, and $\gamma = \frac{1}{4}$), the scheme is second-order accurate in time, but weakly damped π oscillations of the spurious modes are present.

A typical choice for a first-order Newmark method is the scheme with parameters $\alpha = \frac{1}{2}$, $\beta = 1$, and $\gamma = 0$. This scheme is the fully implicit Newmark scheme. The eigenvalues are then $\lambda_2 = 0$ and $\lambda_3 = -K/(K + 2)$. Again, one of the spurious modes has weakly damped π oscillations.

Let us consider now the schemes for which $\beta + \gamma = 1$. The eigenvalues for these schemes are $\lambda_2 = 0$ and $\lambda_3 = (\alpha - 1)K/(1 + \alpha K)$, which reduces to $\lambda_3 = (\alpha - 1)/\alpha$ for large values of K. One of the spurious modes is damped immediately. For $\alpha < \frac{1}{2}$, the scheme is unstable. For $\frac{1}{2} \leq \alpha < 1$, the other spurious mode is oscillatory damped. For $\alpha = 1$, all spurious modes are immediately damped. For $\alpha > 1$, the other spurious mode is supercritically damped (without oscillations).

Several schemes are tested in the results section to show the validity of this analysis. The scheme with $\alpha = \beta = 1$ and $\gamma = 0$ will finally be used for the computations. This scheme corresponds to the first-order backward Euler scheme and corresponds to the time-integration scheme for the fluid problem. Note that for another choice of the time-integration scheme for the fluid problem the analysis should be repeated and will have an impact on the choice of the integration scheme for the solid problem. Also note that for small K, close to zero, the spurious modes are damped very well, independent of the choice of α, β, and γ. Thus, if only a weak coupling exists between the fluid and the solid problems, the matching of the time-integration scheme for both problems is of less importance.

Stability of the Subiteration Process

In more general applications, the system given by Eq. (13) is solved in an iterative way because no closed expression for the force in function of the solid variables is available. The force is obtained from a CFD computation, as is done for the valve motion, shown later in this paper. A subiteration process can be set up as follows. Starting from an approximation for the new acceleration $\ddot{x}^{n+1,k}$, new values for the velocity $\dot{x}^{n+1,k}$ and the position $x^{n+1,k}$ are computed with the time-integration scheme for the solid. Here k is the subiteration index, starting at 0. The new position is then passed to the fluid problem, where the force $F^{n+1,k}$ is computed. From the equation of motion (6), a newer value for the acceleration $\ddot{x}^{n+1,k+1}$ is then computed, and the cycle is repeated until convergence is achieved.

Let us first consider only schemes for which, when entering the fluid problem, the velocity computed in the fluid problem $\dot{x}_{\mathrm{NS}}$ is equal to the velocity in the solid problem $\dot{x}$. From Eqs. (9) and (11), it can be deduced that the conditions for the parameters are $\beta + \gamma = 1$ and $\alpha = \beta$. The backward Euler scheme belongs to this family of schemes, but none of the schemes of the Newmark family does. For these particular schemes, we can write the equation of motion for the generic test case (10) as

$$\ddot{x}^{n+1} = K\left\{[1/(1-a)][(u^{n+1} - u^n)/\Delta t] - (\alpha\ddot{x}^{n+1} + \gamma\ddot{x}^n)\right\} \tag{25}$$

so that the discrete solution of the acceleration on the new time level is given by

$$\ddot{x}^{n+1} = [K/(1 + \alpha K)][1/(1-a)][(u^{n+1} - u^n)/\Delta t] - [\gamma K/(1 + \alpha K)]\ddot{x}^n \tag{26}$$

However, Eq. (25) cannot be solved directly for $\ddot{x}^{n+1}$ in a more general application as already explained but has to be solved iteratively.

Explicit Coupling in the Subiterations

If explicit coupling in the subiteration process is used, $\ddot{x}^{n+1,k+1}$ is computed as

$$\ddot{x}^{n+1,k+1} = (1 - \omega)\ddot{x}^{n+1,k} + \omega K\{[1/(1-a)] \times [(u^{n+1} - u^n)/\Delta t] - (\alpha\ddot{x}^{n+1,k} + \gamma\ddot{x}^n)\} \tag{27}$$

With $\ddot{x}^{n+1,k} = \ddot{x}^{n+1} + \ddot{\varepsilon}^{n+1,k}$, where $\varepsilon^{n+1,k}$ is the error in the subiteration process with respect to the discrete solution $\ddot{x}^{n+1}$, Eq. (27) can be written as

$$\ddot{\varepsilon}^{n+1,k+1} = -(1 - \omega - \omega\alpha K)\ddot{\varepsilon}^{n+1,k} \tag{28}$$

The amplification of the error is determined by

$$|\varepsilon^{n+1,k+1}/\varepsilon^{n+1,k}| = |1 - \omega - \omega\alpha K| \tag{29}$$

The amplification factor is less than one if

$$\omega < 2/(1 + \alpha K) \tag{30}$$

For small gaps, an unusual small ω is required, close to zero. The amplification factor is zero for ω given by

$$\omega = 1/(1 + \alpha K) \tag{31}$$

The error is then equal to zero after one subiteration. However, this approach is not suitable for flows where the dimension of the gap changes with time as for opening and closing valves. Then it would be more appropriate to use an implicit coupling method in the subiterations.

Implicit Coupling in the Subiterations

A way to have implicit coupling in the subiterations is to compute $\ddot{x}^{n+1,k+1}$ from

$$m\ddot{x}^{n+1,k+1} = F^{n+1,k+1} \approx F^{n+1,k} + \frac{\partial F}{\partial \ddot{x}}(\ddot{x}^{n+1,k+1} - \ddot{x}^{n+1,k}) \tag{32}$$

For the generic test case, the derivative $\partial F/\partial \ddot{x}$ is given by $\partial F/\partial \ddot{x} = -mK$. The error $\ddot{\varepsilon}^{n+1,k+1}$ is defined by

$$\ddot{\varepsilon}^{n+1,k+1} = -K\ddot{\varepsilon}^{n+1,k} - K(\ddot{\varepsilon}^{n+1,k+1} - \ddot{\varepsilon}^{n+1,k}) \tag{33}$$

which results in $\ddot{\varepsilon}^{n+1,k+1} = 0$. Therefore, the amplification factor is equal to zero, independent of the gap size and the fluid and solid densities.

The derivative has to be evaluated numerically in more general applications. This can be done as follows:

$$\frac{\partial F}{\partial \ddot{x}} = \frac{F_{\mathrm{NS}}(\ddot{x}^{n+1,0} + \Delta\ddot{x}) - F_{\mathrm{NS}}(\ddot{x}^{n+1,0})}{\Delta\ddot{x}} \tag{34}$$

Two extra Navier–Stokes (NS) evaluations per time step are needed with this approach to evaluate the derivative. Note that the acceleration variables in this equation are those of the solid problem because the acceleration variables are first used to compute new positions x with the time integration scheme and the forces F_{NS} are evaluated with these positions. Thus, the latter approach can be used to converge the subiterations for any value of the parameters α, β, and γ. This approach is used with success for the moving valve problem, as is shown later.

FSI of an Aortic Valve

Problem Definition

To verify the numerical behavior of the coupling procedure a two-dimensional representation of the aortic valve configuration is considered (Fig. 2). The model contains an inflow tract (inlet corresponds with left ventricle), a sinus of Valsalva (aortic valve), an outflow tract (outlet corresponds with aorta), and a rigid leaflet. The dimensions of the model are $l_1 = 4$ cm, $l_2 = 4$ cm, $r_1 = 2$ cm, $r_2 = 0.7$ cm, $h = 2$ cm, and $\theta_{\mathrm{initial}} = 0.384$ rad $= 22$ deg. The flow during the ejection phase (systole) is computed. As boundary conditions (Fig. 3), a pulsatile aortic flow in x direction is given as a function of time at the inlet.

For $0 < t < t_0$ and $t_0 + 0.37\,T_p < t < T_p$,

$$v_{\mathrm{inlet}} = v_{\mathrm{jump}} + 0.5 v_{\mathrm{amp}} \sin\left\{\frac{2\pi[(t - t_0)/T_p + 0.26]}{1.26}\right\} \tag{35a}$$

For $t_0 < t < t_0 + 0.37\,T_p$,

$$v_{\mathrm{inlet}} = v_{\mathrm{jump}} + v_{\mathrm{amp}} \sin\left[\frac{2\pi(t - t_0)/T_p}{0.74}\right] \tag{35b}$$

The parameters in formula (35) are $T_p = 2.45$ s, $t_0 = 0.4$ s, $v_{\mathrm{jump}} = 0.04$ m/s, and $v_{\mathrm{amp}} = 0.11$ m/s. The tangential velocity at the inlet is set equal to 0 m/s. At the outlet, a constant gauge pressure of 0 Pa is assumed. On all of the other walls, no-slip conditions are defined.

The unknown variables of the problem are the velocity components in x and y direction and the pressure p, together with the coordinates (x, y) of the valve nodes determined by the angle θ.

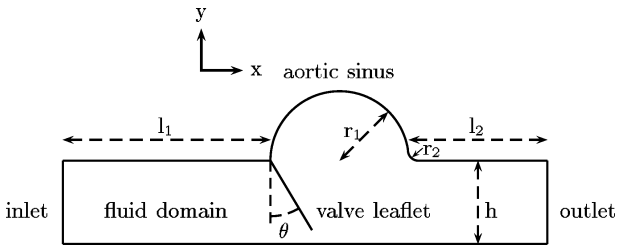

Fig. 2 Geometry of two-dimensional aortic valve model.

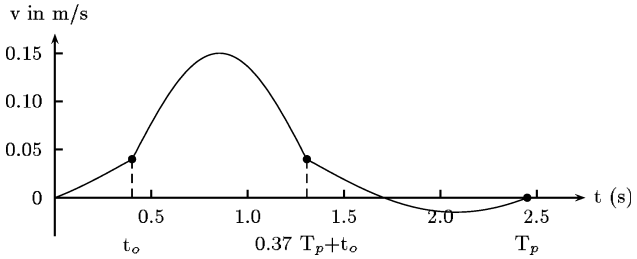

Fig. 3 Velocity boundary condition at inlet as a function of time *t*.

The two-dimensional NS equations for unsteady flow written in a conservative ALE formulation for incompressible laminar fluid flow are solved together with the continuity equation for each moving grid cell in the flow domain. Water ($\rho_f = 1000$ kg/m^3 and dynamic viscosity $\mu = 1$ mPa · s) and blood ($\rho_f = 1000$ kg/m^3 and dynamic viscosity $\mu = 4$ mPa · s) are used in the calculations. Both are treated as a Newtonian fluid. The computation is performed with the dynamic mesh model in the CFD software package FLUENT (Fluent, Inc.). As input, the new position of the boundary nodes of the moving valve has to be prescribed at the beginning of a time step. The dynamic mesh model assumes that grid nodes are connected with springs and an equilibrium equation for the spring forces determines the position of the nodes at the new time level. Between time steps, a local remeshing technique is used to keep a sufficient grid density during the movement of the valve. The positions of the boundary nodes at the new time level are prescribed through a user-defined function (UDF) that can be coupled with the code. Because these positions depend on the FSI solution, a straightforward calculation is not possible. Therefore, a journal file with commands to be executed, is used to drive the computation.

It is necessary to include read and write commands for the geometry and data files in this journal file because it should be possible to start over each time step several times during the coupling procedure. The backward Euler scheme is used in FLUENT for the time integration of the flow problem.

The equation of motion for the stiff valve leaflet is written as

$$M = I\ddot{\theta} \tag{36}$$

with M the moment resulting from the forces acting on the surface of the leaflet, I the moment of inertia, and θ the angle that determines the position of the leaflet as indicated in Fig. 2. For the valve leaflet, the moment of inertia I with the rotational axis at the end of the leaflet is given by

$$I = \left(\tfrac{1}{3}\right) m l^2 \tag{37}$$

with $m = \rho l t$ the mass of the leaflet per unit length, ρ the density of the leaflet (1100 kg/m^3), t the thickness of the leaflet (1 and 0.5 mm) and l the length of the leaflet (22 mm). A reference length of 1 m is used in the third dimension, corresponding to the reference length used in the CFD package to calculate the moments. Both values for the moment of inertia I, 3.909 and 1.9545 kg mm^2, are used.

Implementation of FSI

Figure 4 is a flow diagram of the coupling of the flow computations and the movement of the leaflet. The flow diagram corresponds to the method with implicit coupling in the subiterations. In the following paragraphs the different steps of the implementation are explained. First, all UDF variables t, Δt, n, k, I, θ, $\dot{\theta}$, and $\ddot{\theta}$ are initialized. The subsequent position of the valve leaflet on the new time level is calculated by coupling the time-integration scheme for the solid with the CFD code. The time-integration scheme for the solid is given by

$$\begin{aligned}\dot{\theta}^{n+1} &= \dot{\theta}^n + (1-\beta)\Delta t\ddot{\theta}^n + \beta\Delta t\ddot{\theta}^{n+1} \\ \theta^{n+1} &= \theta^n + \Delta t\dot{\theta}^n + \gamma\Delta t^2\ddot{\theta}^n + \alpha\Delta t^2\ddot{\theta}^{n+1}\end{aligned} \tag{38}$$

The indices $n+1$ and n correspond with time levels $t + \Delta t$ and t, respectively.

Iterative Solution of the Backward Euler Method

To obtain the position θ^{n+1} at $t + \Delta t$, an iterative approach is used. For each time step there are k subiterations performed to reach sufficient convergence of Eq. (36).

At the beginning of each time step, the derivative $\mathrm{d}M/\mathrm{d}\ddot{\theta}$ has to be estimated. A first estimation ($k = 0$) of the new position $\theta^{n+1,k=0}$ is computed with the old value of the angular acceleration $\ddot{\theta}^n$. This value of the acceleration is used to calculate the position using Eq. (38). With this initial guess of the new position at $t + \Delta t$,

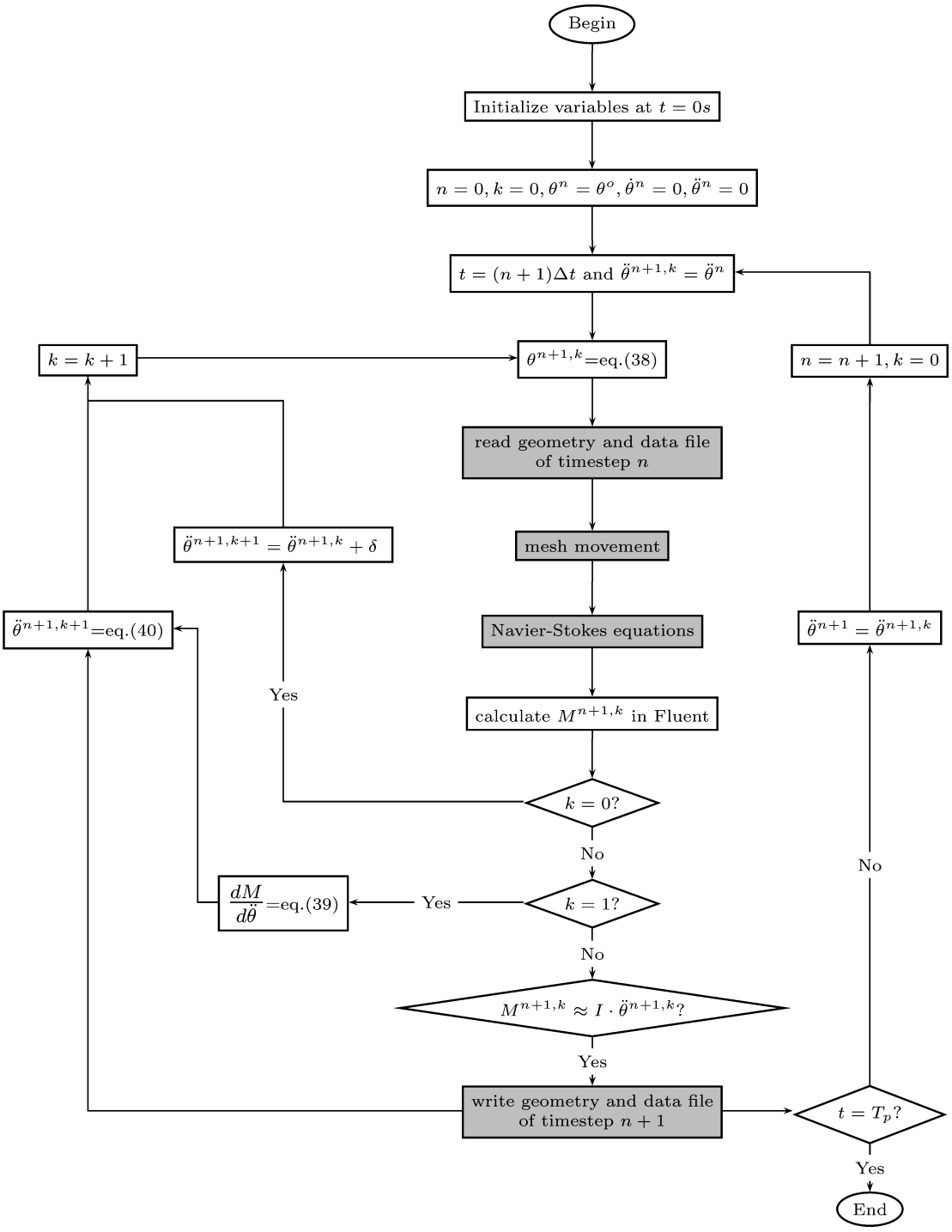

Fig. 4 Flow diagram of coupling of fluid and structure in FLUENT: n = time step, k = subiteration step, and $\delta = 0.1$ rad/s^2: shaded, Fluent, Inc., software executed using generated journal file and unshaded, UDFs executed using generated journal file.

FLUENT is called to adapt the mesh with the dynamic mesh model and to solve the NS equations. After convergence of the NS equations, $M^{n+1,k=0}$ is calculated. A second estimation ($k = 1$) of the new position $\theta^{n+1,k=1}$ is computed with the old value of the angular acceleration increased with a constant $\delta = 0.1$ rad/s^2. This value is about 1/100 of the maximum angular acceleration, which can be estimated from the inlet profile. It is shown that the choice of this value is not very sensitive. After convergence of the fluid problem, $M^{n+1,k=1}$ and the derivative $\mathrm{d}M/\mathrm{d}\ddot{\theta}$ are calculated as follows:

$$\ddot{\theta}^{n+1,k=0} = \ddot{\theta}^n, \qquad \ddot{\theta}^{n+1,k=1} = \ddot{\theta}^n + \delta$$

$$\frac{\mathrm{d}M}{\mathrm{d}\ddot{\theta}} = \frac{M^{n+1,k=1} - M^{n+1,k=0}}{\ddot{\theta}^{n+1,k=1} - \ddot{\theta}^{n+1,k=0}} = \frac{M^{n+1,k=1} - M^{n+1,k=0}}{\delta} \tag{39}$$

The derivative $\mathrm{d}M/\mathrm{d}\ddot{\theta}$ can now be used to calculate a better approximation of the position of the valve leaflet:

$$M^{n+1,k+1} = I\ddot{\theta}^{n+1,k+1}$$

$$\Downarrow$$

$$M^{n+1,k} + \frac{\mathrm{d}M}{\mathrm{d}\ddot{\theta}}(\ddot{\theta}^{n+1,k+1} - \ddot{\theta}^{n+1,k}) = I\ddot{\theta}^{n+1,k+1}$$

$$\Downarrow$$

$$\ddot{\theta}^{n+1,k+1} = \frac{[M^{n+1,k} - (\mathrm{d}M/\mathrm{d}\ddot{\theta})\ddot{\theta}^{n+1,k}]}{(I - \mathrm{d}M/\mathrm{d}\ddot{\theta})} \tag{40}$$

With this better approximation of the angular acceleration, the new position is calculated, the mesh is adapted, and the NS equations are solved. After convergence of the NS equations, $M^{n+1,k}$ is calculated and convergence of the inner loop is checked:

$$M^{n+1,k} \approx I\ddot{\theta}^{n+1,k}$$

The inner loop is repeated until convergence is achieved. A convergence criterium of a residual drop of three orders of magnitude is used. Then the next time step is computed. If only one cycle is computed, the simulation ends at $t = T_p$.

Results and Discussion

Solution of the Problem

Figure 5 shows the meshed geometry. It is shown in Fig. 5 that the ALE remeshing requires at least one cell in the gap between the valve leaflet and the wall. Thus, the valve will never close completely. However, the gap can be made as small as required by local refinement of the mesh. The backward Euler time-integration scheme for the solid has been used, unless stated otherwise.

First a grid convergence study is performed. This study is done with water as fluid, with a time step of 1 ms and with a moment of inertia $I = 3.909$ kg mm^2. Three grids are considered. The angle of the valve is plotted as a function of time for the first cycle in Fig. 6. The finest grid is further used for all computations.

The influence of the magnitude of the time step is shown in Fig. 7. Here, the computations are done for blood as fluid and for a moment of inertia $I = 1.9545$ kg mm^2. A time step equal to 1/1000 of the interval of the cycle ($\Delta t = 2.45$ ms) is compared with a time step of 1 ms. Both computations give the same result for the movement of the valve. A time step of $\Delta t = 2.45$ ms is further used for all computations, unless specified otherwise.

A convergence study for the cycle is shown in Fig. 8, with the same fluid and moment of inertia. The positions of the valve at the beginning and the end of the third cycle correspond to each other, and the positions of the valve during the second-half of the second cycle correspond with those of the third cycle (Fig. 8a). The pressure differences between inlet and outlet are also shown as a function of time in Fig. 8b. No differences can be seen between the different cycles. This pressure difference is, however, less sensitive because it is mainly determined by the velocity profile applied at the inlet, and this is the same for all cycles. The pressure difference plot (Fig. 8b) shows two discontinuities at $t = t_0$ and at $t = t_0 + 0.37T_p$. This is because the inlet velocity also has this discontinuity in its derivative (Fig. 3). We conclude that, from the third cycle on, the differences between the cycles can be assumed to be negligible. This discontinuity would not have been present for a smoother inlet profile. However, if a strong acceleration is present in the inlet profile during a short-time interval and if a time step is used that does not resolve this time interval, then the same problem would arise.

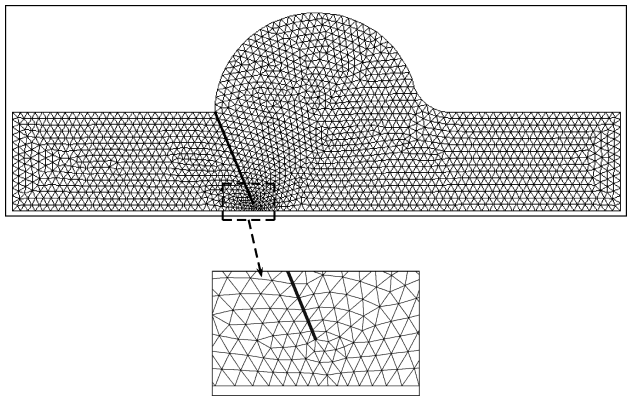

Fig. 5 ALE grid of two-dimensional aortic valve model.

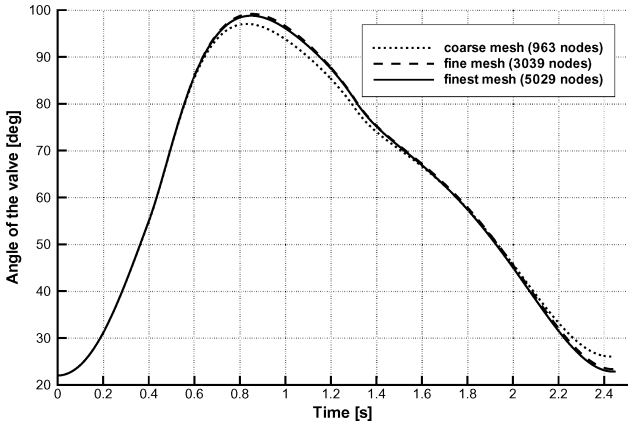

Fig. 6 Comparison of evolution of angle of valve for different grids densities.

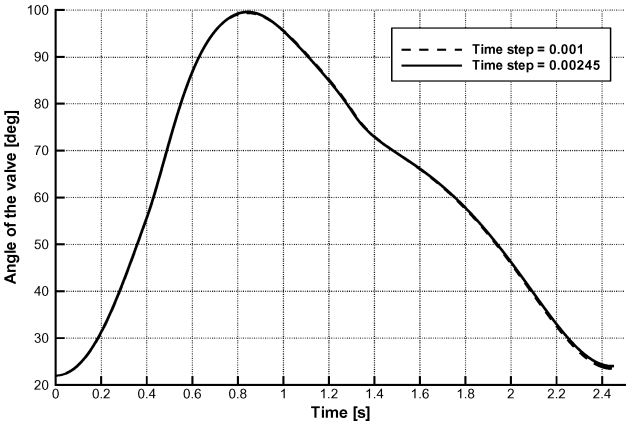

Fig. 7 Comparison of evolution of angle of valve for two different time steps.

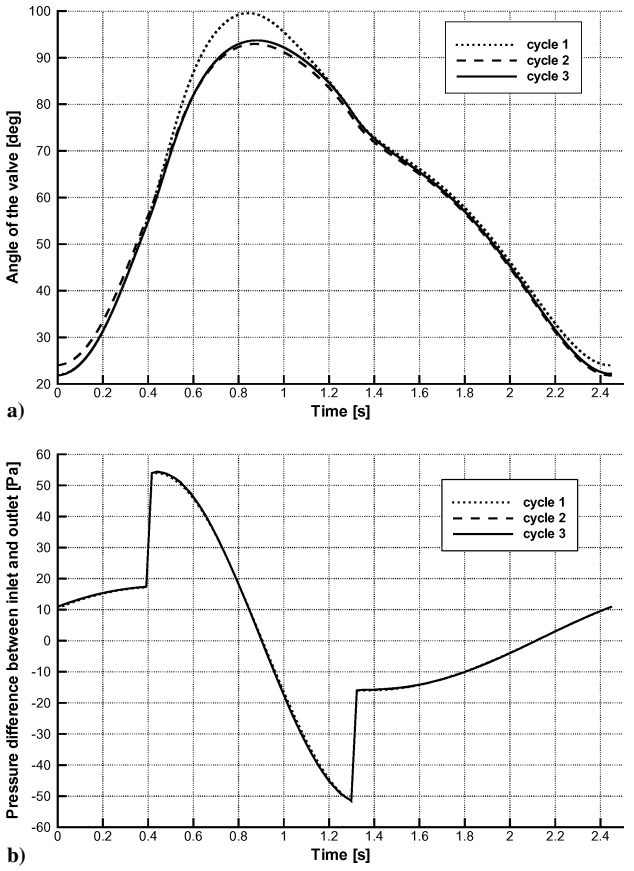

Fig. 8 Evolution of angle of valve and pressure difference between inlet and outlet for first three cycles.

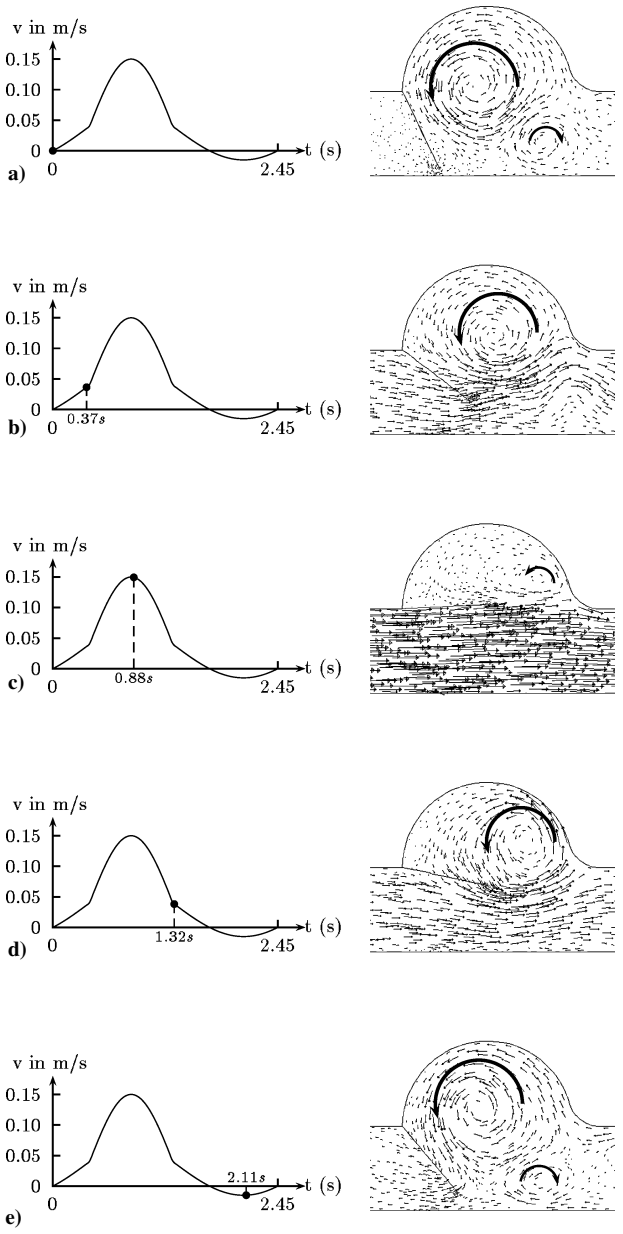

Fig. 9 Velocity vectors for t = a) 0.00, b) 0.37, c) 0.88, d) 1.32, and e) 2.11 s.

At this point, spurious modes can enter the solution. These should be damped immediately. The inlet profile that is used introduces a spurious mode independent of the size of the time step. Thus, with this inlet profile, the damping behavior for spurious modes of the different numerical schemes can be tested.

Figure 9 shows the velocity vectors at five different moments in time during the flow cycle. The arrows show how the vortices are changing during the cardiac cycle. Figure 9 shows that the opening and closing of the valve can be computed with the presented method. It is clear that the backflow plays an important role in the closing of the aortic valve: in the converged cycle, the valve reaches the closed state because of the presence of a period during which backflow is present at the inlet boundary. We will further focus on the numerical behavior of the FSI problem; the application itself is not further discussed. Some applications are addressed in Refs. 8 and 9.

Stability of the Time-Integration Scheme

The conclusions of the stability analysis on the generic one-dimensional test case are numerically verified with the moving valve problem. The analogy between the two problems has been already mentioned. The main difference between the one-dimensional test case and this two-dimensional problem is the difference in the length of the gap. In the one-dimensional test case, it is assumed that only the acceleration of the fluid in the gap is responsible for the pressure difference across the solid. The influence of the two-dimensional effects at both ends of the gap is neglected. In the two-dimensional problem of the valve, the length of the gap is negligible. The pressure difference between both sides of the valve is now not only due to the acceleration of a small amount of fluid in the gap, but also the acceleration of fluid in front of and behind the gap must be taken into account. This influence cannot be quantified easily, but it is not necessary. It is clear that the amount of fluid that must be accelerated is much greater than only the amount of fluid in the gap. This means that the factor K is not equal anymore to the expression given in Eq. (14), but much larger. Also note that when the valve reaches the open state a gap exists between the main flow and the fluid in the sinus of Valsalva. Therefore, the one-dimensional test case problem is representative for most of the cycle during opening and closing of the valve, and especially in the completely closed and open positions.

Table 1 Explicit stepping, $\alpha = \beta = \gamma = 0$ and $\Delta t = 0.001$ s

Time	θ, rad	$\dot{\theta}$, rad/s	$\ddot{\theta}$, rad/s^2
0.000	0.3840	0.00	0.00
0.001	0.3840	0.00	284.91
0.002	0.3841	0.28	−4,971.54
0.003	0.3819	−4.69	96,525.94
0.004	0.4255	91.84	−5,054,412.89

Table 2 Explicit stepping, $\alpha = \beta = \gamma = 0$ and $\Delta t = 0.00001$ s

Time	θ, rad	$\dot{\theta}$, rad/s	$\ddot{\theta}$, rad/s^2
0.00000	0.383972000	0.000000	0.00
0.00001	0.383972000	0.000000	269.71
0.00002	0.383972013	0.002697	−4,319.77
0.00003	0.383971824	−0.040501	71,972.37
0.00004	0.383975018	0.679223	−1,193,827.07

Table 3 Damping of the spurious modes for different schemes

	$\ddot{\theta}$, rad/s^2[a]		
Scheme	$t = 0.00245$ s	$t = 0.00490$ s	$t = 0.00735$ s
	Newmark, $\gamma = \frac{1}{2} - \alpha$		
$\alpha = \frac{1}{4}$, $\beta = \frac{1}{2}$	29.201	−26.191	51.106
$\alpha = \frac{1}{2}$, $\beta = 1$	14.963	0.413	14.577
$\alpha = 0.4$, $\beta = 0.6$	18.604	5.101	1.415
	$\beta = 1$, $\gamma = 0$		
$\alpha = 0.4$	18.604	−8.418	30.842
$\alpha = 0.5$	14.963	0.413	14.577
$\alpha = 0.6$	12.533	4.354	9.706
$\alpha = 0.8$	9.449	7.121	7.709
Backward Euler	7.576	7.587	7.592
$\alpha = 1$			
$\alpha = 1.5$	5.077	6.751	7.312

[a]In the subiterations, $\ddot{\theta}$ is converged.

Tables 1 and 2 show the evolution of the angle, the angular velocity, and the angular acceleration during the first four time steps of the first cycle for an explicit time integration scheme ($\alpha = \beta = \gamma = 0$) for the motion of the solid. Two time steps are compared: $\Delta t = 1$ ms and $\Delta t = 0.01$ ms. Blood is used as fluid, and the moment of inertia $I = 3.909$ kg mm^2.

The explicit scheme is unstable. The spurious modes are more or less amplified in the same way in both calculations independent of the time step. This behavior is predicted by the stability analysis.

For the calculations in the rest of this paragraph, blood is used as fluid, the time step $\Delta t = 2.45$ ms, and moment of inertia $I = 1.9545$ kg mm^2 are used.

In Table 3, some Newmark schemes, the backward Euler scheme, and some of the other ($\beta = 1$, $\gamma = 0$) schemes are tried out. The angular acceleration of the first three time steps of the first cycle are given. The backward Euler scheme gives a critically damped behavior and can be treated as a reference for the other schemes. In

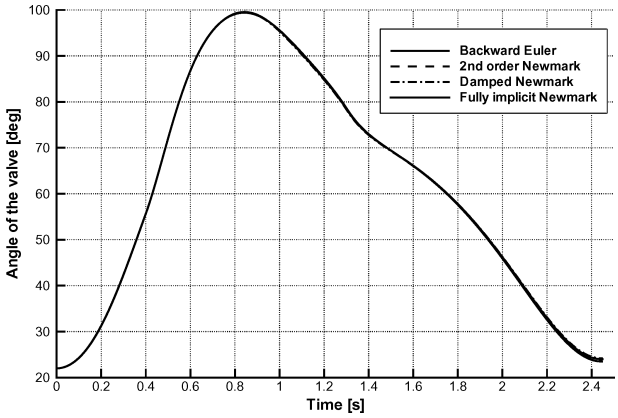

Fig. 10 Comparison of evolution of angle of valve for first cycle computed with backward Euler scheme, second-order Newmark scheme, fully implicit Newmark scheme, and damping Newmark scheme, $\alpha = 0.4$ and $\beta = 0.6$.

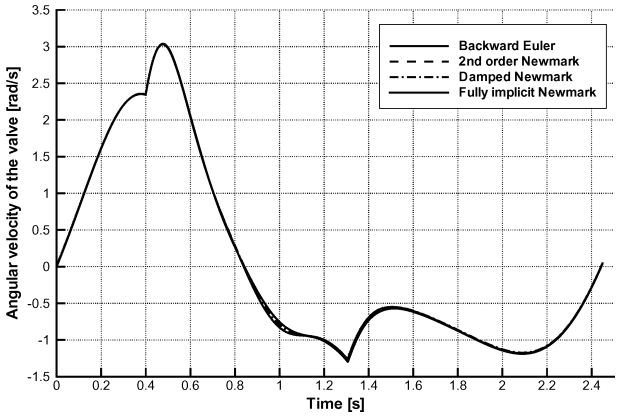

Fig. 11 Comparison of evolution of angular velocity of valve for first cycle computed with backward Euler scheme, second-order Newmark scheme, fully implicit Newmark scheme, and damping Newmark scheme, $\alpha = 0.4$ and $\beta = 0.6$.

Figs. 10–12, the angle, the angular velocity and the angular acceleration computed with the backward Euler scheme, the second-order Newmark scheme ($\alpha = \frac{1}{4}, \beta = \frac{1}{2}$), the fully implicit Newmark scheme ($\alpha = \frac{1}{2}, \beta = 1$), and a damping Newmark scheme ($\alpha = 0.4, \beta = 0.6$) are shown as a function of time for the complete first cycle.

With Table 3 and Figs. 10–12, part of the conclusions of the stability analysis for the generic one-dimensional test case is verified. The second-order Newmark and the fully implicit Newmark scheme show almost no damping. The damping of the ($\beta = 1, \gamma = 0$) schemes also behaves as was predicted. For $\alpha = 0.4$, the scheme is unstable; for $\alpha = \frac{1}{2}$, the scheme is weakly damped; and for $\alpha = 0.6$ and $\alpha = 0.8$, the scheme gives subcritical damping for the spurious modes with an oscillatory behavior. For $\alpha = 1$, the backward Euler scheme is obtained, which gives critical damping for the spurious modes. They are damped immediately. For $\alpha = 1.5$, a supercritical damping behavior is seen. Agreement with the stability analysis is obtained for all of these tests.

In Table 4, the convergence of the subiteration process is analyzed for one time step of the backward Euler scheme. The analysis is done at time level $t = 2.695$ s. This time level is chosen because at this point the convergence behavior of the subiteration process is the worst compared with the rest of the cycle. At this time level, the angle of the valve is 0.6612 rad (37.89 deg). The difference between the moment computed with the CFD software and $I\ddot{\theta}$ is given for the first four subiterations. When the implicit approach is used in the subiterations, the first two subiterations are used to calculate the derivative.

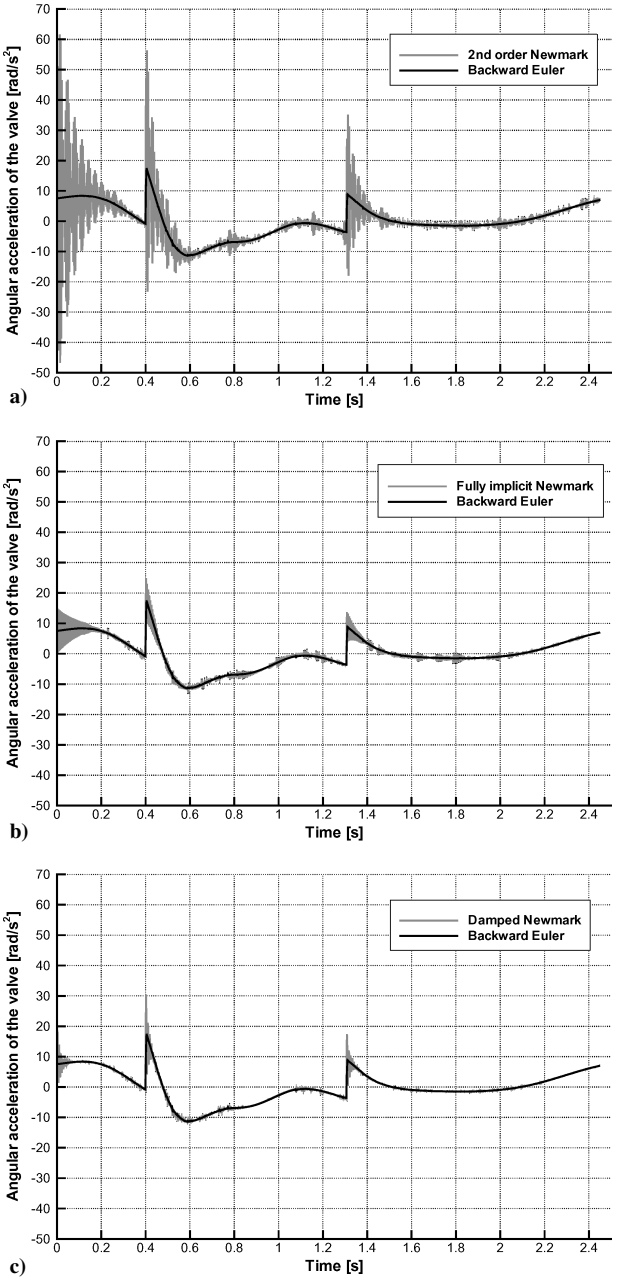

Fig. 12 Comparison of evolution of angular acceleration of valve for first cycle computed with backward Euler scheme, second-order Newmark scheme, fully implicit Newmark scheme, and damping Newmark scheme, $\alpha = 0.4$ and $\beta = 0.6$.

With explicit coupling in the subiterations, no convergence could be obtained.

For an underrelaxation factor $\omega = 0.025$, a good damping is obtained; a value $\omega = 0.05$ leads to divergence; and for a value $\omega = 0.005$, almost no damping of the subiteration process is obtained. This shows the sensitivity to the underrelaxation factor. Because the factor K changes during the opening and the closing process, a good value for the whole cycle could not be obtained.

The method that uses the derivative of the force with respect to the angular acceleration shows good damping for a broad range of values of δ, defined in Eq. (39). This value determines the displacement of the valve in the second step of the subiteration cycle. This displacement should be less than the size of the grid cells in the vicinity of the valve. We used a value of $\delta = 0.1$ rad/s^2 because it is almost 1/100 of the maximum acceleration present in the problem. This maximum acceleration can be estimated from the inlet boundary condition in our application. Another way to choose δ is to use a

Table 4 Behavior of error of subiterations for backward Euler scheme ($\alpha = \beta = 1, \gamma = 0$)[a]

	$M_{CFD} - I\ddot{q}$, N · m				
Method	Subiteration 1	Subiteration 2	Subiteration 3	Subiteration 4	Remark
Explicit	4.918E−04	1.177E−02	3.378E−01	Crash	Diverging
$\omega = 0.05$	1.119E−05	1.583E−05	2.313E−05	3.360E−05	Diverging
$\omega = 0.025$	1.121E−05	2.431E−06	5.2670E−07	1.148E−07	
$\omega = 0.005$	1.123E−05	8.493E−06	6.428E−06	4.865E−06	Very slow
$\delta = 10^{-7}$ rad/s^2	Calculation of $\partial F/\partial\ddot{\theta}$		1.2944E−05	6.2502E−04	Diverging
$\delta = 0.001$ rad/s^2	Calculation of $\partial F/\partial\ddot{\theta}$		1.3294E−05	3.0894E−08	
$\delta = 0.1$ rad/s^2	Calculation of $\partial F/\partial\ddot{\theta}$		1.122E−05	3.740E−07	
$\delta = 1$ rad/s^2	Calculation of $\partial F/\partial\ddot{\theta}$		1.122E−05	7.142E−07	
$\delta = 100$ rad/s^2	Calculation of $\partial F/\partial\ddot{\theta}$		1.3294E−05	3.0894E−08	
$\delta = 100{,}000$ rad/s^2	Calculation of $\partial F/\partial\ddot{\theta}$ crashes				Crash

[a]Time level $t = 2.695$ s.

fraction of the current angular acceleration. The value must then be prohibited to become too small if the angular acceleration becomes close to zero. For too small values of δ, the difference between the two moments from which the derivative is computed becomes too small and is of the same size or even smaller than the error on the computed moments. The magnitude of this error depends on the accuracy of the solution of the NS problem. We used a residual drop of three orders of magnitude as a convergence criterion for the fluid solver. In Table 4, it is shown that a too small value of δ leads to a crash of the calculation for this reason. If δ is taken too large, the displacement that corresponds with it is also too large, and the moving mesh solver diverges, which explains the crash in this situation. The choice of δ is application dependent but not very sensitive, which makes the method robust.

The behavior of the subiteration process also matches the behavior predicted in the generic one-dimensional test problem.

Validation

Several validation studies of the algorithm have been performed. In Ref. 8 the method is compared with the measurements in an experimental setup in which the flow is nearly two-dimensional. Good agreement is found (max. error about 10%). In Ref. 9 the method is applied to a real three-dimensional valve, and comparison is made with the experimental study of Feng et al.[10,11] The opening and closing behavior is also here in good agreement. It could be shown that depending on the geometry behind the valve, the opening and closing behavior of the valve is influenced in agreement with the Feng study.

Conclusions

This study shows a stability analysis for FSI problems in which different fluid zones are almost separated by a moving rigid body but connected through gaps in the vicinity of the moving rigid body. A FSI calculation procedure is constructed that couples the movement of a rigid body with the flow calculations performed in a commercial CFD package. The procedure is succesfully applied to the opening and closing of a two-dimensional model for the aortic valve.

From the stability analysis and the numerical experiments, it can be concluded that the matching of the time-integration scheme for the fluid and the solid problem is very important for these kinds of FSI problems. It has been shown that, for a backward Euler scheme used in the fluid problem, a backward Euler scheme for the solid problem damps all of the spurious modes of the coupling procedure immediately. The second-order Newmark scheme and the fully implicit Newmark scheme show a weakly damped behavior. Other schemes with good damping behavior can be constructed. The stability analysis showed also that, for loosely coupled FSI problems, the matching of the numerical scheme for the fluid and the solid problem is much less important to damp the spurious modes.

A second conclusion is that the convergence of the subiteration process also deserves a lot of attention for these kinds of FSI problems. A standard underrelaxation technique does not work well because the choice of the underrelaxation factor is very sensitive to the amount of stiffness of the coupling. Because this stiffness is not necessarily constant during a calculation, such a method is not robust. The use of an implicit coupling procedure in the subiterations, with the use of a numerically computed derivative, which acts as a sensitivity parameter, leads to a robust method to tackle these stiff FSI problems.

Acknowledgment

Kris Dumont is a recipient of Grant IWT-SB-3117 of the Flemish Institute for the Promotion of Scientific–Technological Research in Industry.

References

[1]Lemmon, J. D., and Yoganathan, A. P., "Three-Dimensional Computational Model of Left Heart Diastolic Function with Fluid–Structure Interaction," *Journal of Biomechanical Engineering*, Vol. 122, No. 2, 2000, pp. 109–117.

[2]Peskin, C. S., and McQueen, D. M., "Modeling Prosthetic Heart Valves for Numerical Analysis of Blood Flow in the Heart," *Journal of Computational Physics*, Vol. 37, 1980, pp. 113–132.

[3]Baaijens, F. P. T., "A Fictitious Domain/Mortar Element Method for Fluid–Structure Interaction," *International Journal for Numerical Methods in Fluids*, Vol. 35, No. 7, 2001, pp. 743–761.

[4]De Hart, J., Peters, G. W. M., Schreurs, P. J. G., and Baaijens, F. P. T., "A Two-Dimensional Fluid–Structure Interaction Model of the Aortic Valve," *Journal of Biomechanics*, Vol. 33, No. 9, 2000, pp. 1079–1088.

[5]De Hart, J., Peters, G. W. M., Schreurs, P. J. G., and Baaijens, F. P. T., "A Three-Dimensional Computational Analysis of Fluid–Structure Interaction in the Aortic Valve," *Journal of Biomechanics*, Vol. 36, No. 1, 2003, pp. 103–112.

[6]Makhijani, V. B., Yang, H. Q., Dionne, P. J., and Thubrikar, M. J., "Three-Dimensional Coupled Fluid–Structure Simulation of Pericardial Bioprosthetic Aortic Valve Function," *ASAIO Journal*, Vol. 43, No. 5, 1997, pp. M387–M392.

[7]Wood, W. L., *Practical Time-Stepping Schemes*, Oxford Univ. Press, New York, 1990, pp. 51–61.

[8]Dumont, K., Stijnen, M., Vierendeels, J., van De Vosse, F., and Verdonck, P. R., "Validation of a Fluid-Structure Interaction Model of a Heart Valve Using the Dynamic Mesh Method in Fluent," *Computer Methods in Biomechanics and Biomedical Engineering*, Vol. 7, No. 3, 2004, pp. 139–146.

[9]Dumont, K., Vierendeels, J., Segers, P., Van Nooten, G., and Verdonck, P. R., "Predicting ATS Open Pivot Heart Valve Performance with Computational Fluid Dynamics," *Journal of Heart Valve Disease*, Vol. 14, No. 3, 2005, pp. 393–399.

[10]Feng, Z., Umezu, M., Fujimoto, T., Tsukahara, T., Nurishi, M., and Kawaguchi, D., "In Vitro Hydrodynamic Characteristics Among Three Bileaflet Valves in the Mitral Position," *Artificial Organs*, Vol. 24, No. 5, 2000, pp. 346–354.

[11]Feng, Z., Nakamura, T., Fujimoto, T., and Umezu, M., "In Vitro Investigation of Opening Behavior and Hydrodynamics of Bileaflet Valves in the Mitral Position," *Artificial Organs*, Vol. 26, No. 1, 2002, pp. 3–39.

K. Ghia
Associate Editor